Available online at www.sciencedirect.com

SciVerse ScienceDirect

Ceramics International 38 (2012) 1779–1783

CERAMICS INTERNATIONAL

www.elsevier.com/locate/ceramint

Novel side dams including advanced laminated ceramic for twin roller continuous casting

Zehua Zhou *, Zehua Wang, Yu Yi, Shaoqun Jiang, Gang Wang, Jiangbo Cheng

College of Mechanics and Materials, Hohai University, Nanjing, Jiangsu 210098, China

Received 14 September 2011; received in revised form 28 September 2011; accepted 29 September 2011
Available online 6 October 2011

Abstract

Novel side dams for twin roller continuous casting were fabricated. The side dams were divided into three zones and were prepared with different materials to meet working demands. Al_2O_3–ZrO_2 laminated ceramic was used as a key part to overcome immense friction and wear and frequent thermal impact during the whole casting process. A series of experiments for laminated composite were carried out, and the results indicated that the laminated composite presents rather excellent comprehensive properties including considerable fracture strength and fracture toughness, high critical thermal shock temperature difference and good tribological properties. These superior comprehensive properties are mainly attributed to the special laminated structure with expected residual stress in different layers. Furthermore, the side dams were successfully applied in the twin roller continuous casting in the laboratory. The side dams exhibit good working ability under extremely tough conditions and the steel strips produced by continuous casting present good qualities.

Keywords: B. Interfaces; C. Thermal shock resistance; C. Wear resistance; E. Structural applications

1. Introduction

Twin roller continuous casting, a sort of near-net-shape technology, presents numerous advantages on economical production of thin strips, such as low energy consumption, low equipment and operating costs, and rapid solidification [1–8]. The schematic illustration of twin roller continuous casting is shown in Fig. 1a, and side dams in contact with the rollers act as un-replaceable roles on keeping molten metal from leakage in whole casting process.

Side sets for containing molten metal of twin roller continuous casting can be divided into two kinds, one is electromagnetic dams (EMD), and the other is solid side dams [7,8]. However, high cost of electromagnetic equipment and potential danger once equipments being out of good condition are both considerable factors for EMD, especially for experimental research. Thus, our research is focused on the solid side dams.

During casting process, molten metal is frequently dumped into pool region surrounded by rollers and dams, along with rolls rotate to drag metal strips (see Fig. 1a). So side dams have to suffer extremely tough working conditions such as iterative thermal impact (especially more than 1000 °C for steel and iron), heavy abrasion against rolls and strips at high temperature, as well as erosion from different molten metals. Therefore, for side dams it is necessary to have good combinations of properties including excellent thermal shock resistance associated with wear- and erosion-resistance. So far, research on materials for side dams is seldom reported [7–10]. And in the earlier working, we have experimented tens of stuffs such as high temperature ceramics and refractory materials for side dams, unfortunately no solo commercial material was successfully found out. (Some materials can be used as the dams only in a rather limited times, generally one or several casting processes).

In our present study, by analyzing working conditions in different locations of the dam sheets, we divided the sheets into three zones (see Fig. 1b), accordingly designed novel composite dam sheets including both ceramic and refractory materials. The mechanical properties, thermal shock resistance and wear resistance of the key zone made of Al_2O_3–ZrO_2

* Corresponding author.
E-mail address: zhouzehua0011@yahoo.com.cn (Z. Zhou).

0272-8842/$36.00
doi:10.1016/j.ceramint.2011.09.064

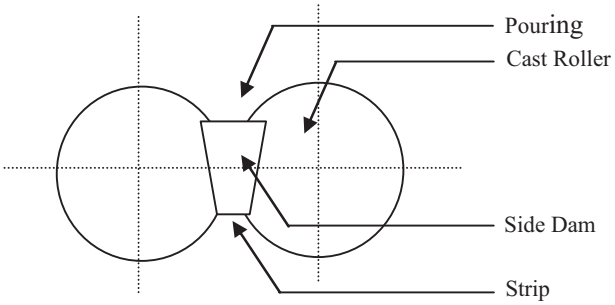

a) Schematic of twin roller continuous casting

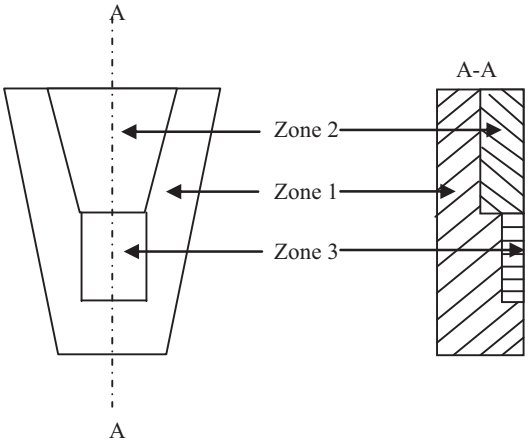

b) Structural diagram of novel side dam set

Fig. 1. Schematic illustration of twin roller continuous casting and structural diagram of novel side dam set.

laminated ceramic were investigated, as well as the ceramic was observed and analyzed. Furthermore, the novel side dams were successfully fixed and applied in the twin roller continuous casting equipment.

2. Experimental procedure

2.1. Structural design of side dams

As shown in Fig. 1b, novel side dams were designed, which have three working zones made up of different materials, respectively. Zone 1 is named as ''the substrate'', which is used to hold and fix the zone 2 and zone 3. According to our design, it seldom meet molten metal but may contact rotating rollers during casting process, so excellent strength and wear resistance of it are required, as well as good thermal resistance and low thermal conductivity are also considerable for the reason of thermal insulation. Therefore a sort of asbestos–cement board with a low cost was selected as the substrate. Zone 2, in contrast, which contacts molten metal frequently but does not meet rotating rollers under working condition, was fabricated with fused silica board because of its superior comprehensive properties including excellent thermal shock resistance, thermal insulation and corrosion resistance to molten metal (both asbestos–cement and fused silica material are not further discussed because they are easy to prepare). Zone 3, a key part of the side dams, is always under extremely terrible conditions such as immense friction and wear occurred from frozen metal strips and rollers, and frequent thermal impact of molten metal. Therefore, it must have good high temperature strength and wear resistance, combining with good thermal shock resistance. Besides, it must also exhibit a smooth surface to obtain high-quality strips with regular and smooth edge but without crack and gap. Accordingly, ceramic or ceramic matrix composite is probably the best selection.

Zones 2 and 3 were inlaid into the substrate by using a binder with good high temperature resistance, and then the whole dams were polished to become flat.

In the following section we discuss the ceramic composite which was applied for zone 3.

2.2. Preparation and analysis method of the ceramic composite

It is hard to find out a proper candidate applied for zone 3 due to its extremely rigorous demands on properties described above. Ultimately, a laminated ceramic with excellent comprehensive properties was considered.

ZrO_2 powder with 0.6 μm average particle size (containing 3 mol% Y_2O_3 as sintering stabilizer) and Al_2O_3 powder with 0.5 μm average particle size (containing 0.5 wt% MgO as sintering aid) were selected to prepare laminated composite. The composite includes two surface layers and one center layer, and the thickness of them are $d_1 = 0.3 \pm 0.1$ mm and $d_2 = 5.4 \pm 0.2$ mm, respectively. So the total thickness of the composites d is 6.0 ± 0.4 mm (see Fig. 2).

In order to obtain residual compressive stress in the surface layers (The reason will be discussed later), 5 wt% $Al_2O_3 + ZrO_2$ in the center layer and 30 wt% $Al_2O_3 + ZrO_2$ in the surface layers were selected, respectively (actually series of both laminated and un-laminated composites with different compositions were studied, but they are not the point of this paper and here we just study the best one in the whole series).

The composite powders were dry-pressing molded at room temperature using a 60 T double-pressing machine. Then the compacts were sintered at 1620 °C for 90 min in air.

The critical thermal shock temperature difference ΔT_c under a quick cooling condition was tested by the residual fracture strength method [11]. Different temperatures (ΔT) from 150 to 600 °C with an interval of 50 °C were designed.

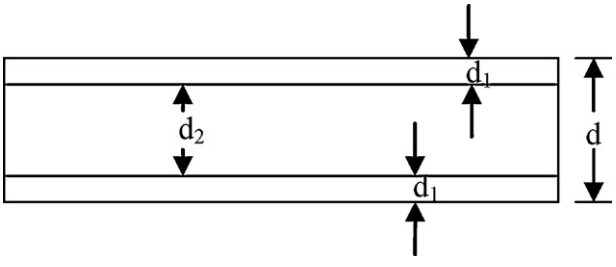

Fig. 2. Schematic of three-layer composites.

Table 1
Residual strength after thermal shock at different temperature.

	Temperature/°C										
	0	150	200	250	300	350	400	450	500	550	600
Fracture strength/MPa	786	769	754	741	719	691	670	654	621	545	506

Friction and wear behaviors were investigated using a block-on-ring tester under a dry friction condition with different loads. The tests were performed with a 200 rev/min rotational velocity of the ring, and the time for each test was 10 min. The ceramic blocks with surface roughness $R_a = 0.24$ μm were 4 mm × 6 mm × 30 mm in dimensions. As a couple, a steel ring with $R_a = 0.32$ μm was 40 mm in outer diameter, 16 mm in inner diameter and 10 mm in thickness.

The density D of the composite was measured according to Archimedes method. The fracture strength was tested by standard bending test, and the fracture toughness was determined by the indentation method.

In our experiments, every final value mentioned above was an average result from 5 tested values.

X-ray stress analyzer was used to measure the residual stress of the laminated ceramics. 5 different locations with a 5 mm interval in the surface were measured.

SEM was used to observe the morphologies of the laminated composite.

3. Results and discussion for laminated composite

3.1. Density and mechanical properties

The average density of the composite is about 5.785 g cm^{-3} after sintering, corresponding to 99.01% of the calculated relative density (the theoretical density of the composite was determined by mixture-law), which means the fabricating process is available.

The fracture strength and fracture toughness of the composite are 786 MPa and 18.4 MPa $m^{1/2}$, respectively. The composite with the laminated structure exhibits excellent comprehensive mechanical properties.

3.2. Critical thermal shock temperature difference ΔT_c

Table 1 indicates that ΔT_c of the laminated composite is 500 °C. Obviously, the result is rather striking for engineering ceramics. (In our early study, the best ΔT_c was only 350 °C for the un-laminated composite with a similar composition. More details please refer to [12].)

3.3. Tribological properties

Friction coefficient and wear rate of the composite under a dry friction condition with different loads were investigated and the results are listed in Table 2. It should be emphasized that the dry friction environment without any lubrication were considered only because it is similar to the working condition of the side dams.

The results revealed the friction coefficients of 0.24–0.46 and the wear rates of 1.09–1.35 × 10^{-15} m^3 N^{-1} m^{-1} are relatively low, and no any change appeared on the sample's surface. The composite exhibits an excellent wear resistance. (The reason is not the point in this paper and more detail please refer to [13].)

3.4. Residual stress

Because of great atomic number of Zr and limitation of test, we measured residual compressive stress only 10 μm depth below the surface. The average residual stress is −144 MPa, which indicates that compressive stress exists in the surface layers.

In accordance with the experimental purpose, both compressive stress in the surface layers and tensile stress in the center layer are expected, and they can be obtained through thermal mismatch due to different linear expansion coefficients α between layers after sintering. Thus, by calculating and changing the compositions of different layers, α of surface layer could be always lower than that of center layer.

The residual compressive stress of the composite results consequently in a high toughness, because it not only brings a restricted phase transformation of the tetragonal ZrO_2 grain at the cooling period of sintering, but also counteracts the stress concentration of main cracks to some extent [14,15]. Therefore, it is a key point that this kind of composite was selected as a material for zone 3.

3.5. SEM morphology

The SEM micrographs of the laminated composite are shown in Fig. 3. It is clear that the wave interface exists between two layers (see Fig. 3a) and it is attributed to the special

Table 2
Friction coefficient and wear rate of laminated composites under dry friction condition with different loads.

	Load/N			
	100	200	300	400
Friction coefficient	0.46	0.39	0.30	0.24
Wear rate/×10^{-15} m^3 N^{-1} m^{-1}	1.35	1.38	1.24	1.09

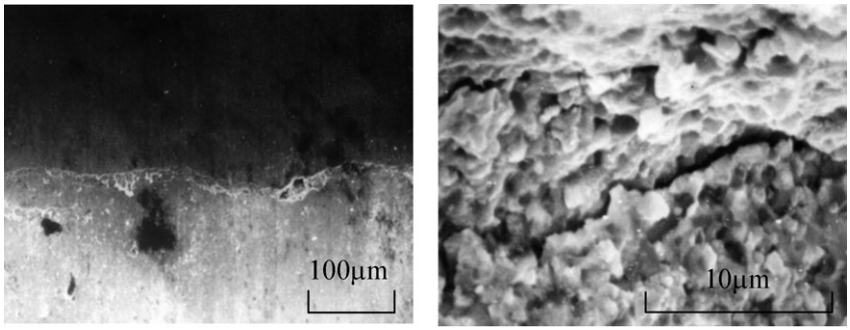

a) Wave interface b) Crack's deflexion in the interface

Fig. 3. SEM morphologies of laminated composite.

pressing routine. Moreover, the crack's deflexion in the interface is observed in Fig. 3b, which means that more energy was consumed by crack's extension and the toughness of composites was improved accordingly [14–16].

Fig. 4 shows the surfaces of the composite after wear with different loads. Evidently, the surfaces became gradually coarse with the increasing loads, and soft plastically deforming strips occurred and became severe at 300 N and 400 N load condition, respectively. It could be concluded that adhesive wear resulted from plastic deformation is a main mechanism, and usually it does not result in an abrupt failure of materials. Besides, no crack was found on the surface after wear. Therefore, by combining tribological properties and SEM morphology, it could be determined the laminated composite has a good wear resistance under the fry friction condition.

4. Applying validations of side dams on twin roller continuous casting mechanism

The side dams were installed on the SLB-1 test continuous casting mechanism with ϕ250 mm twin rollers in the laboratory. Si steel and 18–8 stainless steel were molten at more than 1500 °C and then were poured into the mechanism, respectively. Casting time was also considered, including both single time and multi times casting with about 15 min intervals. Both quality of the steel strips and competence of the side dams are considerable. No failure even crack and corrosion but only a bit of slight wear on the surface of the side dams occurred, and the surfaces of them were still smooth even if after more than ten times' casting. Moreover, the steel strips present good qualities with rather greatly smooth edge and no burr on them.

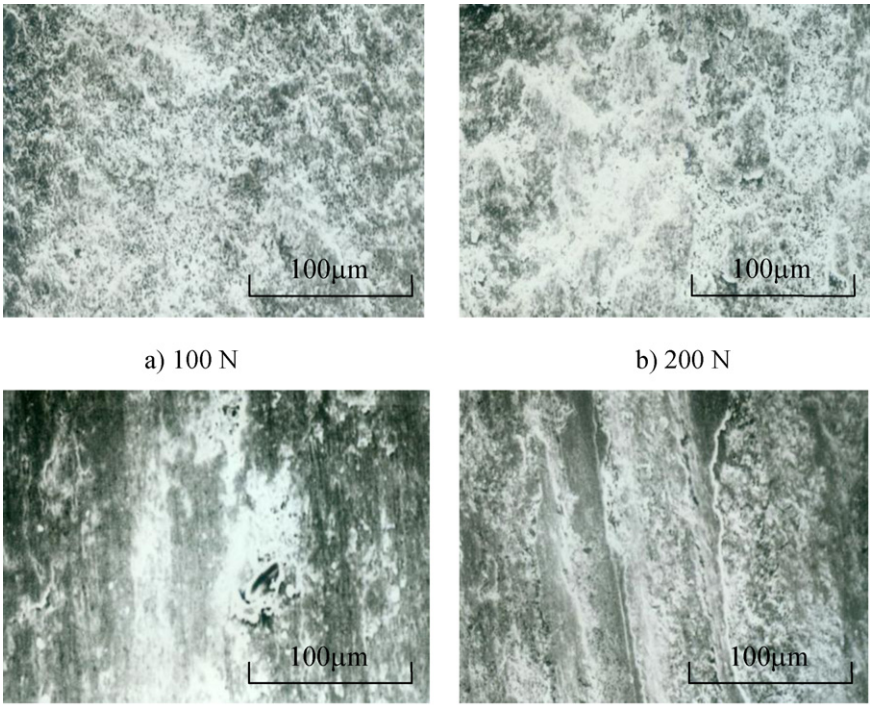

a) 100 N b) 200 N

c) 300 N d) 400 N

Fig. 4. Surface SEM morphologies of laminated composite after wear with different loads.

Therefore, the side dams prepared with the structure and materials, which are cost-effective and easily controllable manufacturing process compared with electromagnetic dams, can become a good candidate used in twin roller continuous casting mechanism.

5. Conclusions

Novel side dams for twin roller continuous casting were successfully fabricated. The side dams were divided into three zones according to different working conditions and were prepared with different materials to satisfy working demands. The laminated ceramic with excellent comprehensive properties was used as a key part because it always met extremely terrible conditions including immense friction and wear and frequent thermal impact during casting process. Correspondingly, the mechanical properties, thermal-shock resistance and tribological properties as well as micro-structure of the laminated composite were investigated.

The results indicated that the laminated composite exhibits excellent comprehensive properties. The fracture strength and fracture toughness are 786 MPa and 18.4 MPa $m^{1/2}$, respectively. The critical thermal shock temperature difference is over 500 °C, and the friction coefficients of 0.24–0.46 and the wear rates of $1.09–1.35 \times 10^{-15}$ m^3 N^{-1} m^{-1} are relatively low under the dry friction condition. The superior comprehensive properties are mainly due to the special laminated structure with expected residual stress in different layers.

The side dams were successfully applied in the twin roller continuous casting in the laboratory. The side dams exhibited good working ability under extremely tough conditions. Moreover, the steel strips produced by continuous casting present good qualities. Thus, it is hopeful the novel side dams can become a good candidate used in twin roller continuous casting mechanism.

Acknowledgements

This work is supported by the Foundation of Innovative Talent, Hohai University (No. 26, 2009, Hohai University) and the Fundamental Research Funds for the Central Universities (Grant No. 2009B15914) and Scientific Research Startup Fund of HoHai University (Grant No. 2084/40801117).

References

[1] H. Toshio, T. Kenta, I. Masaaki, W. Hisaki, Twin roll casting of aluminum alloy strips, J. Mater. Process. Technol. 153–154 (2004) 42–47.
[2] M. Yun, D.J. Monagham, X. Yang, J. Jang, et al., An experimental investigation of the effect of strip thickness, metallostatic head and tip setback on the productivity of a twin-roll caster, Cast Met. 4 (1991) 108–111.
[3] D.V. Edmonds, J.D. Hunt, D.J. Monagham, X. Yang, M. Yun, An experimental study of twin-roll casting, in: Proceedings of the Extraction Refining and Fabrication of Light Metals, CIM, Ottawa, 1991, pp. 257–271.
[4] H. Toshio, Semisolid strip casting using a twin roll caster equipped with a cooling slope, J. Mater. Process. Technol. 130–131 (2002) 558–561.
[5] C.H. Gras, M. Meredith, J.D. Hunt, Microstructure and texture evolution after twin roll casting and subsequent cold rolling of Al–Mg–Mn aluminium alloys, J. Mater. Process. Technol. 169 (2005) 156–163.
[6] R. Wechsler, The status of twin roll casting technology, Scand. J. Metall. 32 (2003) 56–62.
[7] H.L. Wang, X. Yan, Z.S. Lei, J.M. Gu, Z.M. Ren, K. Deng, Study on side containment technology of twin-roll thin strip continuous casting, Steelmaking 23 (2007) 54–58.
[8] K.E. Blazek, W.F. Praeg, J.G. Rachford, Commercial-scale verification of the feasibility of electromagnetic edge containment for the twin rol1 strip casting of steel, Iron Steelmak. 25 (1998) 39–45.
[9] P. Fournier, F. Platon, Laboratory wear studies of refractory side dams in the strip steel casting process, Tribol. Interf. Eng. Series 39 (2001) 167–175.
[10] P. Fournier, F. Platon, Wear of refractory ceramics against nickel, Wear 244 (2000) 118–125.
[11] Test method for thermal shock resistance of high performance ceramics. Chinese Standard, GB/T 16536-1996.
[12] Z.H. Zhou, Z.H. Wang, Y. Yi, S.Q. Jiang, J.S. Lan, A thermal-shock-resistance model for laminated ceramics and its validation, J. Eur. Ceram. Soc. 30 (2010) 1543–1547.
[13] Z.H. Zhou, P.D. Ding, S.H. Tan, J.S. Lan, ZrO_2–Al_2O_3 laminated ceramics and their tribological behaviors, Surf. Rev. Lett. 12 (2005) 75–84.
[14] R. Bermejo, J. Pascual, T. Lube, R. Danzer, Optimal strength and toughness of Al_2O_3–ZrO_2 laminates designed with external or internal compressive layers, J. Eur. Ceram. Soc. 28 (2008) 1575–1583.
[15] T. Lube, J. Pascual, F. Chalvet, G. Portu, Effective fracture toughness in Al_2O_3–Al_2O_3/ZrO_2 laminates, J. Eur. Ceram. Soc. 27 (2007) 1449–1453.
[16] S. Sarkar, B. Lee, Evaluation and comparison of the microstructure and mechanical properties of fibrous Al_2O_3–(m-ZrO_2)/t-ZrO_2 composites after multiple extrusion steps, Ceram. Int. 36 (2010) 1971–1976.